Rovedar

Journal of Lab Animal Research. 2026; 5(1): 1-14.

DOI: 10.58803/jlar.v5i1.88

http://jlar.rovedar.com/

Original Article

Clinical Pathology of Renal Amyloidosis in a Captive Population of Tree Shrews (*Tupaia belangeri*)

Natalie Steiner[1,2*], Tina Brezina[1,3], Felix Felmy[4], Frederik Kiene[4], Yara Silberstein[4], Malgorzata Ciurkiewicz[5], Andreas Beineke[5], Jan Hinrich Bräsen[6], Reinhold Paul Linke[7], Claudia Busse[8], Michael Pees[1], Ute Radespiel[4], and Maximilian Reuschel[1]

[1] Department of Small Mammal, Reptile and Avian Medicine and Surgery, University of Veterinary Medicine Hannover, Foundation, Hannover, Germany

[2] Institute for Terrestrial and Aquatic Wildlife Research (ITAW), University of Veterinary Medicine Hannover, Foundation, Busum, Germany

[3] Center for Animal Health, Baden-Baden, Germany

[4] Institute of Zoology, University of Veterinary Medicine Hannover, Foundation, Hannover, Germany

[5] Department of Pathology, University of Veterinary Medicine Hannover, Foundation, Hannover, Germany

[6] Nephropathology Unit, Institute of Pathology, Hannover Medical School, Hannover, Germany

[7] Reference Center of Amyloid Diseases, amYmed, Munich, Germany

[8] Department of Small Animal Medicine and Surgery, University of Veterinary Medicine Hannover, Foundation, Hannover, Germany

* ***Corresponding author***: Natalie Steiner, Department of Small Mammal, Reptile and Avian Medicine and Surgery, University of Veterinary Medicine Hannover, Foundation, Hannover, Germany. Institute for Terrestrial and Aquatic Wildlife Research (ITAW), University of Veterinary Medicine Hannover, Foundation, Busum, Germany. Email: natalie.steiner@tiho-hannover.de

ARTICLE INFO

Article History:
Received: 26/12/2025
Revised: 19/01/2026
Accepted: 04/02/2026
Published: 14/02/2026

Keywords:
AA-amyloidosis
Animal model
Protein misfolding
Tupaia belangeri

ABSTRACT

Introduction: Captive tree shrews (*Tupaia belangeri*) are widely used as experimental models for neurological, visual, and infectious disease studies. Despite evidence suggesting a genetic or physiological predisposition to systemic amyloidosis in this species, its clinicopathological characteristics are still poorly understood. The present study aimed to characterize clinicopathological changes associated with systemic amyloidosis in a captive breeding colony of *Tupaia belangeri* (*T. belangeri*) and to explore potential early ante-mortem indicators in blood indices, imaging, or clinical examination of the disease.

Materials and methods: Nineteen *T. belangeri* were included in the present study (seven males, 12 females) with a mean age of 3.3 years from a single institutional breeding colony at the University of Veterinary Medicine Hannover, Germany. Fifteen animals underwent standardized ante-mortem clinical assessment, including physical and ophthalmic examination, serum biochemistry, urinalysis, radiography, and abdominal ultrasonography, followed by necropsy and histopathology. Four animals were included solely on the basis of pathological and histological examination due to long intervals between the prior clinical evaluation and necropsy. Amyloid was identified histologically by Congo red staining and confirmed as AA-type by immunohistochemistry.

Results: Systemic AA-amyloidosis was detected in 74% of the examined *T. belangeri* (14/19), predominantly affecting the kidneys and intestines. A significant association was observed between renal cysts and amyloid deposition. An association with urine specific gravity was observed, while no significant associations were identified between amyloidosis and other biochemical, urinary, radiographic, or ultrasonographic parameters, nor with sex, body weight, or age.

Conclusion: Systemic AA-amyloidosis appeared to be common in captive *T. belangeri*, predominantly affecting the kidneys and intestine, while lacking reliable ante-mortem clinical or laboratory indicators, highlighting the need for improved diagnostic approaches.

1. Introduction

Cite this paper as: Steiner N, Brezina T, Felmy F, Kiene F, Silberstein Y, Ciurkiewicz M, Beineke A, Bräsen JH, Linke RP, Busse C, Pees M, Radespiel U, and Reuschel M. Clinical Pathology of Renal Amyloidosis in a Captive Population of Tree Shrews (*Tupaia belangeri*). 2026; 5(1): 1-14. DOI: 10.58803/jlar.v5i1.88

Animal models remain indispensable for advancing understanding of human diseases, particularly in areas where *in vitro* methods fall short[1,2]. While the house mouse (*Mus musculus*) dominates preclinical studies due to its genetic tractability and ease of maintenance[3,4], notable differences in immune function and disease progression limit its translational relevance in some contexts[2,3,5]. These limitations in commonly used mouse models have prompted a growing interest in alternative models, including the tree shrew (*Tupaia belangeri*), a small mammal phylogenetically positioned between rodents and primates[6].

Tree shrews offer several advantages as experimental models, including their neuroanatomy and visual cortex organization, which are the shared key organizational features with primates[7], and their small size, short gestation, and year-round breeding make them logistically feasible for laboratory use[8,9]. As a result, *Tupaia belangeri (T. belangeri)* has been utilized in studies of neurobiology[10], infectious diseases[11], and visual disorders[8,9]. However, their broader use in biomedical studies remains limited, in part due to accessibility and incomplete characterization of their health profiles under laboratory conditions[9]. In 1997, a breeding colony of *T. belangeri* was established at the University of Veterinary Medicine Hannover, Germany[12]. Necropsy-based studies in this colony revealed a high prevalence of systemic AA-amyloidosis, affecting 72% of animals, with deposits observed in the kidneys, skin, intestines, and lymph nodes[12]. The kidneys, in particular, demonstrated parenchymal atrophy and cystic degeneration, suggesting potential renal dysfunction[12]. Amyloid deposits have been reported in the brains of aging tree shrews, further indicating a possible species-specific susceptibility[9].

Amyloidosis is characterized by the accumulation of insoluble fibrils in tissues, potentially leading to organ dysfunction[12,13]. There are numerous forms of amyloidosis as well as numerous precursor proteins that are involved in accumulation processes[14]. Among these, AA-amyloidosis is the most common systemic type in animals[15] and is generally linked to chronic inflammation and elevated serum amyloid A (SAA) levels. Systemic AA-amyloidosis has been reported in species such as captive cheetahs, Dorcas gazelles, and California sea lions[13,14]. Another form, familial amyloidosis, refers to systemic AA-amyloid depositions observed in genetically related individuals or lineages[12]. This condition has been documented in several cat breeds, cheetahs, caracals, black-footed ferrets, and brown layer chickens[12,15]. While a genetic or physiological predisposition to amyloid deposition in tree shrews has been proposed, its clinical relevance and underlying mechanisms remain poorly understood[9,15].

The apparent spontaneous development of amyloidosis in *T. belangeri* suggested their potential as a naturalistic model for human protein misfolding diseases such as Alzheimer's disease, Parkinson's disease, and Creutzfeldt-Jakob disease[10]. Additionally, Northern tree shrews as models for protein misfolding diseases could have a valuable impact on veterinary medicine, as amyloidosis has been associated with economic losses in production[13], increased mortality in endangered wildlife species[16], and even interspecies transmission risks[17]. These findings underscored the broader One Health implications of amyloidosis, while also highlighting that the presence of a progressive, potentially debilitating condition within laboratory colonies raises important animal welfare concerns. The present study aimed to explore early clinical parameters associated with systemic AA-amyloidosis in a captive breeding colony of *T. belangeri*, using different non-invasive diagnostic tools such as ultrasonography, serum biochemistry, urinalysis, and ophthalmic examination.

2. Materials and methods

2.1. Ethical approval

All procedures were approved by the local authorities and the animal welfare officer of the University of Veterinary Medicine Hannover, Germany. The study was conducted under license number TiHo-T-2019-16. All principles of laboratory animal care were followed. All relevant international guidelines and regulations were strictly observed.

2.2. Animals

Nineteen tree shrews (seven males and 12 females) with an average age of 3.3 years from a breeding colony at the Institute of Zoology, University of Veterinary Medicine Hannover, Germany, were included in the present study. All animals originated from a single institutional breeding colony; their family relationships are depicted in Figure 1. The animals were kept as single individuals or opposite-sex pairs in mesh cages (150 cm × 150 cm × 80 cm per animal), each with a nesting box and wooden enrichment, including resting shelves and tree branches. The room temperature was maintained at 25±2°C, and the relative humidity was recorded at 50%. Water was offered *ad libitum*, and the diet included Tupaia pellets (Altromin 6020, Altromin International, Lage, Germany), fresh fruits, and insects[8,18]. The medical history and weight development of all 19 individuals were recorded by the staff in monthly intervals.

All 19 animals were examined between January and February in 2021. Eight animals (four females and four males) were euthanized following the initial examination. One animal died without prior clinical signs (number 15, Quanta). The remaining ten animals (seven females and three males) were euthanized after a second, identical examination conducted between May and July 2021. Following euthanasia, all animals underwent a macroscopic pathological examination on site. A histological examination of a standardized set of tissue samples was conducted at the Department of Pathology at the University of Veterinary

Medicine Hannover, Germany. The exact days of examination and dissection are presented in Supplementary Table 1. To assess potential correlations with clinical parameters, only animals examined within 15 days before necropsy (animals number 1-14) were included in the clinicopathological analysis. For animals number 15-19, only pathological findings were evaluated, as the interval between clinical examination and necropsy was considered too long to reliably reflect acute clinical changes.

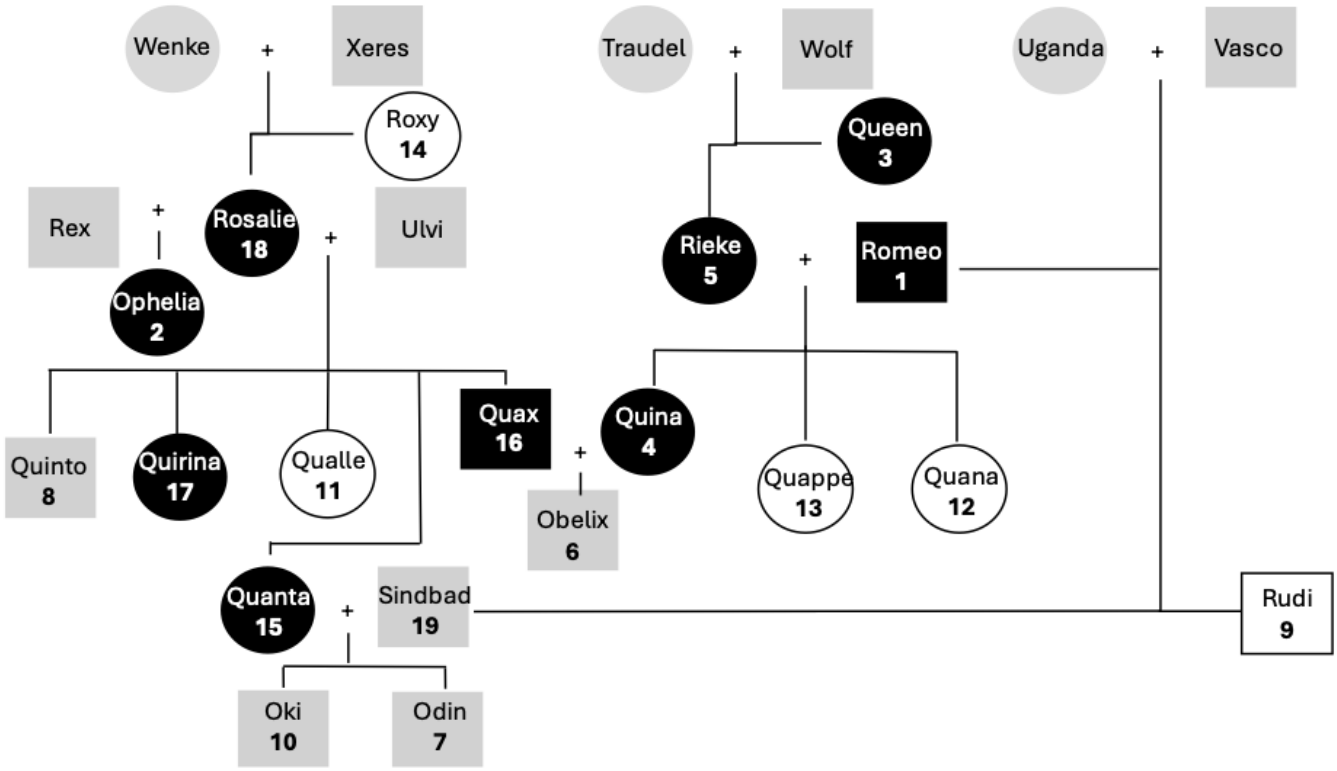

Figure 1. Family tree of the breeding colony of tree shrews (*Tupaia belangeri*) at the Institute of Zoology, University of Veterinary Medicine Foundation Hannover, Germany. Not all individuals shown were included in the present study; animals without identification numbers were incorporated into the pedigree solely to illustrate familial relationships. Circles represent females and squares represent males. Original animal names were used to facilitate interpretation. The numbers of the animals used in the study are written in bold beneath their names. Black-shaded symbols indicate individuals with renal amyloid deposition, white symbols indicate general (non-renal-specific) amyloid deposition, and light-grey symbols represent individuals without detected amyloid depositions.

2.3. Clinical examination

Clinical examination was conducted at the Department of Small Mammal, Reptile and Avian Medicine and Surgery, University of Veterinary Medicine, Hannover, Germany. Each animal was transported to the clinical department, using closed wooden nest boxes, which the animals entered voluntarily due to prior training.

For the examination and diagnostic procedures, the animals were sedated. The animals were anesthetized inside their nest boxes using 5% isoflurane (IsofluranCP, CP-Pharma GmbH, Germany). The *T. belangeri* were then injected intramuscularly with a fully antagonizable anaesthesia, fentanyl at 9.95 µg/kg (Fentadon 50 µg/mL, Dechra Veterinary Products, Germany), medetomidine at 0.1mg/kg (Cepetor 1 mg/mL, CP-Pharma GmbH, Germany), and midazolam at 0.5 mg/kg (Midazolam 5 mg/mL, Group panpharma, Rotexmedica, Germany) in a mixed syringe. The anaesthesia protocol used in the present study was selected based on a review of protocols previously applied in other small mammals, including rats[19], chinchillas[20], rabbits[21], and guinea pigs[22]. The use of the combination and evaluation of anaesthesia has already been discussed in the veterinary study[23]. The *T. belangeri* were weighed in their nest box for dosage calculation.

Inhalation anaesthesia was discontinued and after reaching a status of deep sedation, the diagnostic workup included the listed procedures in the following order including clinical examination, digital radiographs using a Gierth HF 400VA X-ray unit (Gierth X-Ray International GmbH, Rendsburg, Germany) equipped with a Philips flat-panel detector (FFD 50 cm, 44 kV, 1.25 mAs; Philips Medical Systems, Hamburg, Germany) in latero-lateral and ventro-dorsal recumbency, examination of the eyes before drug-induced dilatation of pupils, ultrasound of the abdomen (GE Vivid 7 Dimension, Micro curved array transducer, 5–9 MHz; GE Healthcare GmbH, Solingen, Germany), examination of the eyes after dilatation of pupils, and blood withdrawal (*V. saphena lateralis* or *A. femoralis*, 22 G micro-needle, B.Braun, Melsungen, Germany). Urine samples were either collected via cystocentesis during ultrasound or spontaneously during the introduction of anaesthesia. For the latter, the floor of the nest

box was lined with reversed bubble wrap to create collecting hollows. All animals were placed on a heating pad (except during radiographs), monitored manually (heart rate, respiratory rate, mucosal colour, reflexes), received a subcutaneous bolus of fluids (20 ml/kg Sterofundin ISO, B.Braun, Germany), and oxygen per flow-by method whenever possible. After completing the planned diagnostic steps, the animals received 0.5 mg/kg atipamezole (Revertor 5 mg/ml, CP-Pharma GmbH, Germany) and 0.05 mg/kg flumazenil (Flumazenil Kabi 0.1 mg/ml, Fresenius Kabi GmbH, Germany) subcutaneously in a mixed syringe[20,21] and were released into their cages after a full recovery.

Ophthalmic examination comprised slit lamp biomicroscopy (SL-17; Kowa Company Ltd, Tokyo, Japan), indirect ophthalmoscopy (Heine OMEGA 500, Heine, Optotechnik GmbH & Co. KG, Gilching, Germany), and tonometry, set to lapine (Tonovet®; Icare Finland Oy, Helsinki, Finland). Eyes were examined before and 20-30 minutes following the application of tropicamide (0.5% Mydrum, Bauch + Lomb GmbH, Germany).

Blood samples were analysed using a cobas c 311 biochemical analyser (Roche Germany Holding GmbH, Germany). An amount of at least 500 L was used for the analysis. Kidney markers, including creatinine (mg/dL) and urea (mg/dL), total protein (g/dL), albumin (g/dL), and liver enzymes, such as alanine aminotransferase (ALT, U/L) and aspartate aminotransferase (AST, U/L), were assessed.

Urine was evaluated using Combur 9 test strips (Roche Diagnostics GmbH, Mannheim, Germany) to assess total protein and pH. Urinary density was measured via a refractometer.

Reference values for blood samples were based on previously published values for *T. belangeri*[24-26]. Reference values for urine were obtained from non-human primates, such as rhesus (*Macaca mulatta*) and cynomolgus macaques (*Macaca fascicularis*)[27,28], as no reference values were available for the present species.

The animals were euthanized between 0 and 81 days after clinical examination and subsequently submitted for necropsy. Three animals were euthanized using CO_2 inhalation for subsequent neuroanatomical investigations. Fifteen animals were euthanized with deep isoflurane anaesthesia, then decapitated for brain slice preparation, with no prior clinical signs. One animal (number 15, Quanta) unexpectedly died 84 days after its clinical examination and was found dead in its cage with no prior clinical signs.

2.4. Histopathology and immunohistochemistry

From all animals, tissue samples were collected from the kidneys, liver, muscle tissue, skin, intestine, brain, lungs, esophagus, pancreas, spleen, heart, reproductive organs and eyes, for histological, histochemical, and immunohistochemical analyses. The tissues were fixed in 10% neutral-buffered formalin for at least 24 hours, embedded in paraffin, and sectioned at approximately 2 µm. Hematoxylin and eosin staining was performed on tissue sections, which were then examined under an Olympus BX53 microscope (Olympus Europa SE & Co. KG, Germany), and images were captured using an Olympus DP28 camera (Olympus Europa SE & Co. KG, Germany).

Amyloid deposits were detected by Congo red staining. Severity of amyloidosis and renal cysts was graded following the methodology described by Klein et al.[12]. Zero indicated absence of amyloid deposits, + indicated mild amyloid deposits (scattered in the renal papilla, affecting less than 10% of the renal medulla), ++ indicated moderate amyloid deposits (involving 10-50% of the renal medulla), and +++ indicated severe amyloid deposits (affecting more than 50% of the renal medulla). Renal cysts were graded similarly; absent (0), few or sporadic cysts (+), multiple cysts (++), and numerous cysts associated with marked atrophy of the renal parenchyma (+++).

Tissue sections were processed on an automated platform (Ventana ULTRA, Roche Diagnostics, Germany) for deparaffinization, antigen retrieval, and blocking. Primary antibodies, including mc4 (1:100) and mc29 (1:1000), were applied manually and incubated overnight at 4°C. Subsequent steps, including secondary antibody incubation, chromogen development, and counterstaining, were performed on the automated platform[29]. Negative controls, in which the primary antibody was omitted, were included in all staining procedures, and human tissue with confirmed AA-amyloid deposits served as positive control. Following three washes in phosphate-buffered saline, sections were incubated with HRP-conjugated anti-mouse secondary antibodies (Jackson ImmunoResearch Europe, Cambridgeshire, UK) for 30 minutes at room temperature. Chromogenic detection was performed using 3,3′-diaminobenzidine (Zytomed Systems, Germany) according to the manufacturer's instructions, producing a brown reaction product at sites of antibody binding. Sections were then counterstained with hemalum for 1-2 minutes, dehydrated through graded alcohols, cleared in xylene, and mounted.

Negative controls, which lacked the primary antibodies, were used in all procedures to verify specificity. As positive controls, human tissue samples with confirmed AA-amyloid deposits were used.

2.5. Statistical analysis

2.5.1. Statistical analysis of clinical risk factors

To analyze associations between clinicopathological parameters and renal amyloid deposition, different animal subsets were used based on data availability. Clinicopathological blood and urine parameters, such as weight, creatinine, urea, ALT, AST, total protein, albumin, urine total protein, urine specific gravity (USG), and urine pH, were available only for animals' number 1 to 14; therefore, these were analyzed exclusively in these animals.

Sonographic assessments (presence and severity of

renal cysts, structural renal changes) were likewise conducted only in animals' number 1 to 14, and all analyses involving ultrasonography, such as associations between renal amyloid presence and cyst presence or severity, were restricted to this subset.

Post-mortem evaluations of renal cysts were available for all 19 animals; therefore, analyses investigating associations between renal amyloid presence and cysts detected at necropsy were performed on the full dataset.

Pairwise comparisons were performed with Group A defined as amyloid-positive, consisting of animals with histologically confirmed renal amyloid deposits (9/19), and Group B as amyloid-negative, lacking renal amyloid deposits (10/19).

Continuous variables were analysed using Welch's t-test when normally distributed with unequal variances, and the Wilcoxon rank-sum test when non-normally distributed or ordinal. Categorical two-level variables (amyloid presence, cyst presence, sonographic abnormalities) were analysed using Fisher's exact test. Associations between two ordinal variables (severity scores for amyloid compared to cyst severity) were assessed using Spearman's rank correlation.

For all analyses, test statistics (t, W, S), degrees of freedom where applicable, effect sizes, odds ratios with 95% confidence intervals (95% CI), and p values were reported. P values were adjusted for multiple comparisons using the Holm method, with $p \leq 0.05$ considered statistically significant. Statistical analyses were performed in RStudio (RStudio Team, 2024) using R version 12.1 (R Core Team, version 2024.12.1+563). Data handling and preparation were performed using the dplyr package. Normality testing (Shapiro–Wilk), group comparisons (Welch's t-test or Wilcoxon rank-sum test), and p-value adjustments were implemented using functions from rstatix and base R's stats package. Results tables were exported using the writexl and openxlsx packages.

2.5.2. Heritability estimation of general and renal amyloid deposition

Narrow-sense heritability (h^2) was estimated to assess the potential genetic contribution to amyloid deposition in the studied colony of *T. belangeri*. Heritability was evaluated both for general amyloid deposition across the body and for kidney-specific involvement. A pedigree-based linear mixed-effects model was employed for the analysis.

Pedigree data was utilized to create an additive kinship matrix that illustrates the genetic relatedness among individuals (Figure 1). Two phenotypes were analyzed, including general amyloid deposition in the body and renal amyloid deposition, assessed specifically in the kidneys as a separate semi-quantitative trait.

Linear mixed-effects models were fitted using the lmekin function from the coxme R package[30], with animal ID included as a random effect and the kinship matrix used to partition genetic variance. Narrow-sense heritability was calculated as the proportion of total phenotypic variance attributable to additive genetic effects.

3. Results

3.1. Clinical assessment

The mean body weight of the 14 clinically examined *T. belangeri* was 221 ± 21 g, with females averaging 219 ± 18 g and males 225 ± 24 g. The mean age was 3 years (169 ± 77 weeks), with females averaging 162 ± 55 weeks and males 182 ± 113 weeks. Two individuals (Numbers 8 and 11) were placed on restricted diets due to obesity. Review of medical records indicated previous injuries in two animals (Numbers 2 and 10), and the breeding colony produced 18 litters from five females.

Clinical examination revealed pododermatitis in four animals (4/14, 29%). Two of these individuals additionally demonstrated orthopedic abnormalities such as a healed tibial fracture or reduced stifle mobility. One animal without pododermatitis (1/14, 7%) showed bilateral tibiotarsal swelling, and another exhibited intermittent lameness. Three animals exhibited dental tartar (3/14, 21%), and one (1/14, 7%) displayed rostral tooth abrasion.

Ophthalmic assessment identified trichiasis in 5/14 (36%) animals, in three cases unilateral and in two bilateral. The condition appeared to result from a steep eyelid conformation or mild entropion. No corneal pathology associated with trichiasis was detected. Additional ocular findings included one case of persistent hyaloid artery, one immature cataract with fundic pigment disturbance, and one case of blepharoedema and periocular alopecia of unclear origin. Mean intraocular pressure (IOP) was 17 ± 5 mmHg with no significant side differences.

Blood samples were obtained from all 14 animals, but insufficient volumes (< 500 µL) prevented full analysis in four cases (numbers 2, 7, 10, and 11; Table 1). Compared with established reference values[25], blood parameters in the present study exhibited considerable variability. Elevated creatinine levels were found in 77% of animals (10/14; 95% CI: 46-95%), and elevated urea levels in 42% (5/14; 95% CI: 15-72%). Conversely, ALT levels were below reference values in 82% of cases (11/14; 95% CI: 52-96%), and AST levels were below reference values in all animals. Total protein levels were subnormal in 72% of animals (10/14; 95% CI: 46-90%), while albumin levels were elevated in 40% of samples (5/14; 95% CI: 15-72%; Table 1).

Urine samples were collected by cystocentesis from ten animals, obtained spontaneously from one animal, and attempts were unsuccessful in three animals. Macroscopically, all urine samples appeared normal, with a slight yellow color and no distinctive odor. Chemical analysis revealed no presence of bilirubin, urobilinogen, nitrite, or leukocytes in any sample. Two samples tested positive for glucose, three for ketone bodies, and seven for traces of blood, irrespective of the collection method. PH ranged from 5 to 8, and specific gravity from 1.012 to 1.033.

Protein concentrations measured by dipstick were variable and inconsistent with refractometric total solids (0.0-4.4 g/dL; Table 2).

Radiographic examination revealed liver enlargement in 3/14 (21%) animals, a patchy lung pattern in 2/14 (14%), and subjective mild cardiomegaly in 2/14 (14%).

Ultrasonographic examination identified renal changes in 6/14 (42%) animals, with bilateral changes in four and unilateral changes in two. Renal cysts were detected by ultrasonography in the right kidney of 5/14 animals (40%) and in the left kidney of 3/14 animals (20%). An example of a cyst detected by ultrasonography, along with the corresponding pathological findings, was shown in Figure 2A and Figure 2B. Figure 2C and Figure 2D illustrated a macroscopically unremarkable kidney, with corresponding sonographic images revealing no renal cysts. In most cases, sonographic findings corresponded with histopathology, although several discrepancies were noted (Table 2). Of the five animals with histopathologically confirmed renal cysts, three demonstrated corresponding cysts on ultrasonography. Among the nine animals without cysts or amyloid deposition on pathology, eight had unremarkable sonographic findings. Discrepancies were observed in animals number 5, 8, and 9. In animal number 5, renal cysts were identified histologically but could not be assessed by ultrasound. In animal number 9, an anechogenic structure detected on ultrasound was not confirmed histologically, and in animal number 8, parenchymal changes were observed ultrasonographically without corresponding pathological alterations. An overview of the detection of renal cysts and parenchymal changes associated with amyloid presence is presented in Supplementary Table 2.

Table 1. Blood indices of *Tupaia belangeri* evaluated for clinical parameters associated with the occurrence and severity of amyloid deposition

Animal ID	Group	Creatinine (mg/dL)	Urea (mg/dL)	ALT (U/L)	AST (U/L)	TP (g/dL)	Alb (g/dL)
1	A	0.25	69	8	21	4.8	3.25
2	A	0.5	-	-	-	-	-
3	A	0.32	38	13	29	6.28	3.7
4	A	0.31	47	9	-	-	-
5	A	0.38	66	9	39	5.49	3.19
6	B	0.14	65	14	57	5.76	3.84
7	B	-	26	-	-	6.3	-
8	B	0.2	59	80	64	6.78	4.7
9	B	0.33	47	14	81	4.51	2.59
10	B	0.17	-	32	44	5.27	3.37
11	B	0.32	44	-	-	-	-
12	B	0.23	40	13	13	6.45	3.84
13	B	0.24	61	18	21	5.73	3.33
14	B	0.3	16	6	23	4.86	2.79
Reference values		0.14-0.22	28-51	27-110.2	138.3-258.5	6.51-7.33	2.53-3.17

Reference values: Ma et al.[23]. ALT: Alanine aminotransferase, AST: Aspartate aminotransferase, TP: Total protein, Alb: Albumin. Group A: Animals considered as amyloid-positive based on the presence of amyloid deposits in the kidneys, Group B: Animals considered as amyloid-negative with no renal amyloid deposition. 1-14: Number of animals

Table 2. Urine parameters of *Tupaia belangeri* evaluated for clinical indicators associated with the occurrence and severity of amyloid deposition

Animal ID	Group	USG	TP(g/dl)	pH	Protein	Glucose	Ketone	EC/Hb	Sediment
1	A	1020	2.0	7	+	0	+	++++	Leucocytes, mild bacteria
2	A	1012	0.8	7	0	0	0	+++	Mild erythrocytes, mild leucocytes, mild epithelial cells
3	A	1013	1.0	5	+	0	+	+	Not present
4	A	1015	1.4	8	+	++	0	+++	No abnormalities
5	A	1014	1.4	5	++	0	0	+++	Mild leucocytes, mild epithelial cells
6	B	1028	3.9	5	0	0	0	0	Not present
7	B	1016	0.0	-	0	0	0	0	Moderate epithelial cells
8	B	1023	2.9	6	+	0	+	+++	Mild leucocytes
9	B	1024	2.4	6	+	0	0	0	Mild epithelial cells
10	B	1033	4.4	6	0	0	0	+	Mild erythrocytes, mild epithelial cells
13	B	1019	2.0	7	++	+	0	0	Mild epithelial cells

Urine samples were not available from animals 11, 12, and 14. Reference intervals were derived from non-human primates, specifically rhesus macaques (*Macaca mulatta*) and cynomolgus macaques (*Macaca fascicularis*)[26,27], as no species-specific values for tree shrews were available. USG: Urine specific gravity, TP: Total protein, LC: Leukocyte count, EC: Erythrocyte count, Hb: Haemoglobin. Leucocyte count, nitrite, urobilinogen, and bilirubin are not listed in the table as all the animals tested negative for these values.

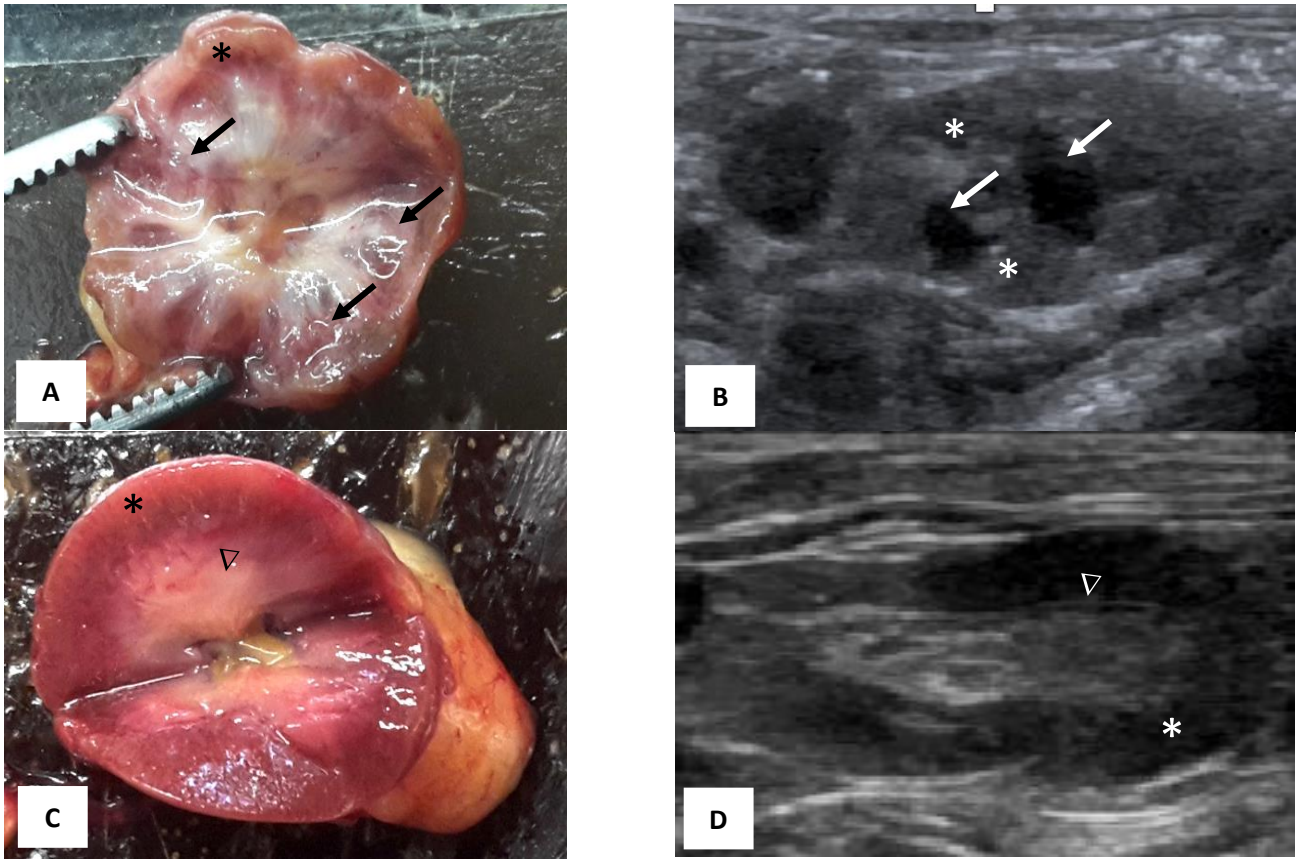

Figure 2. Comparison of gross necropsy and ultrasonographic findings in *Tupaia belangeri* with and without renal pathology. A: Macroscopic image of the kidney from animal number 18, classified as amyloid-positive (Group A), showing severe renal cysts (+++) and severe amyloid deposition (+++). The kidney appears pale with an irregular surface (black asterisk) and multiple cavernous lesions affecting both the cortex and medulla (black arrows). B: Ultrasonographic image of the same kidney (number 18), revealing multifocal anechogenic cystic structures (white arrows), a patchy parenchymal structure (white asterisk), and a loss of distinction between the renal cortex and medulla. C: Macroscopic kidney image of animal number 12, classified as amyloid-negative (Group B), with no evidence of renal cysts or amyloid deposition. The kidney exhibits a smooth surface (black asterisk), a clear corticomedullary distinction (black arrowhead), and no visible cystic lesions. D: Ultrasonographic image of the kidney from animal number 12, showing a homogeneous parenchymal structure (white asterisk) and preserved corticomedullary differentiation (white arrowhead), with no signs of cystic alterations.

3.2. Pathological examination

For pathological examination, all 19 animals were included. Amyloid deposition was identified in 14/19 individuals (74%; 95% CI: 51-88%). Among affected animals, amyloid was most frequently detected in the kidneys of 9/19 (47%; 95% CI: 27-68%) and intestines of 10/19 animals (53%; 95% CI: 32–73%). Less commonly, amyloid was found in the lungs in 1/19 of the *T. belangeri* (5%; 95% CI: 1-25%) and the heart valves in 1/19 (5%; 95% CI: 1–25%). In addition, uterine involvement was observed in 2/12 females (17%; 95% CI: 2-48%). Among the nine animals with renal amyloidosis, six were classified as grade moderate, and two were classified as grade mild, while one animal exhibited severe renal amyloid depositions. Additionally, all nine animals with renal amyloid deposits exhibited renal cysts, with single cysts (+) identified in five animals, multiple cysts (++) in two animals, and numerous (+++) cysts in three animals. One animal exhibited numerous cysts in the kidney, multifocal interstitial fibrosis, and no detectable amyloid deposition (Figure 3).

Amyloid deposits within the kidneys were primarily localized in the medulla and were consistently associated with tubular dilatation in all affected animals (Figure 4). Amyloid deposition in the lamina propria of the small intestine was observed in all cases. Additionally, one animal demonstrated amyloid deposits in the large intestine. Pulmonary deposits were confined to arterial structures, whereas in the heart, amyloid was detected on the valve leaflets. Six animals exhibited lymphohistiocytic interstitial nephritis, but only one had amyloid deposition and a renal cyst. The remaining five animals did not exhibit amyloid deposits. Other pathological findings included granulomatous pneumonia, pulmonary adenocarcinoma, hepatocellular vacuolization, focal interstitial fibrosis in the kidneys, focal purulent myocarditis, ovarian cysts, endometrial hyperplasia, and, in one animal, dysplastic round-cell infiltration in the kidneys, liver, and lymph nodes, with suspicion of malignant lymphoma. Additionally, lymphatic hyperplasia was noted in the spleen. A comprehensive summary of the pathological changes is provided in Supplementary Table 3. Immunohistochemical analysis confirmed that all Congo red–positive amyloid deposits in the kidneys, intestines, lungs, and heart were of the AA type. Negative control sections illustrated no staining, confirming the antibody's specificity.

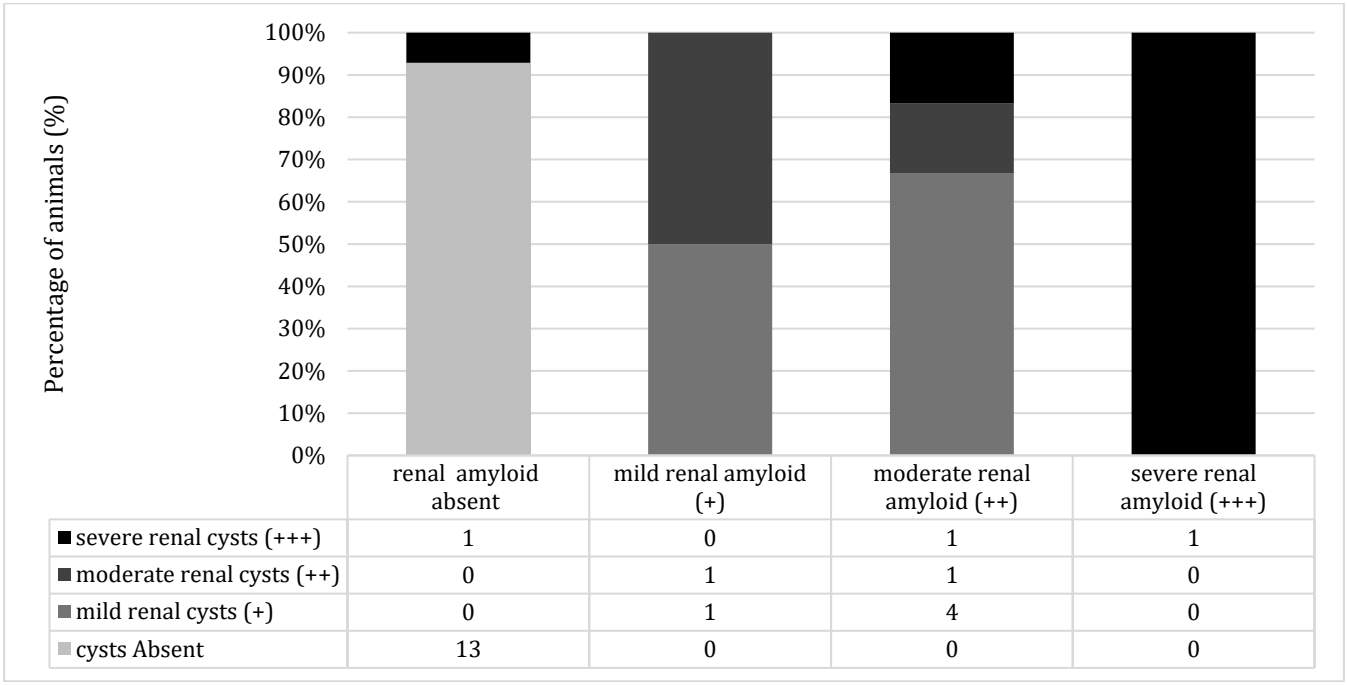

	renal amyloid absent	mild renal amyloid (+)	moderate renal amyloid (++)	severe renal amyloid (+++)
severe renal cysts (+++)	1	0	1	1
moderate renal cysts (++)	0	1	1	0
mild renal cysts (+)	0	1	4	0
cysts Absent	13	0	0	0

Figure 3. Prevalence of renal cysts in relation to the severity of renal amyloid deposition in *Tupaia belangeri.* Data from all 19 animals were included in the analysis.

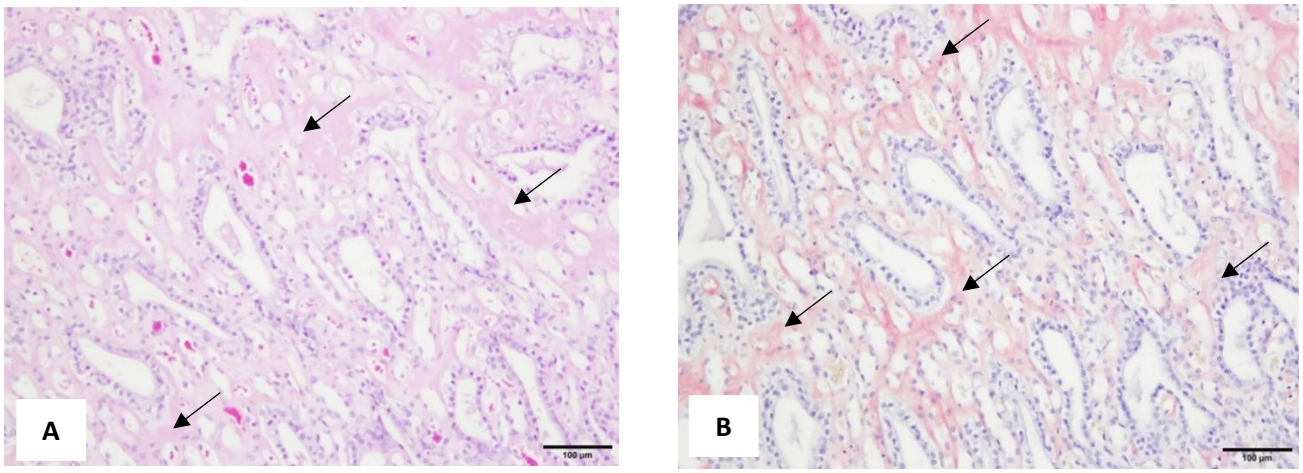

Figure 4. The renal amyloid deposition of *Tupaia Belanger* (animal number 2). A: Renal papilla showing extensive extracellular, glassy, eosinophilic deposits accompanied by marked atrophy of the collecting ducts (black arrows), H&E stain, Scale bar: 100 µm. B: Amyloid deposits within the renal medulla (black arrows), Congo red stain, scale bar: 100 µm.

3.4. Association with clinicopathological changes

All reported p-values were adjusted for multiple comparisons using the Holm method. The present results revealed a significant association between lower USG and the presence of amyloid deposits in the kidney ($p < 0.05$). No other urine, blood, or clinical parameter indicated a significant association. Similarly, no significant associations were observed between renal amyloid deposition and body weight, sex, or age and the presence of amyloid in the kidneys ($p > 0.05$). Creatinine concentrations demonstrated a nonsignificant trend toward higher values in animals with renal amyloid deposition ($p > 0.05$), whereas no other blood parameters were significantly associated after Holm adjustment ($p < 0.05$; Table 3).

No statistically significant associations were detected between renal amyloid deposition and ultrasonographic kidney findings, including cysts or parenchymal alterations ($p > 0.05$). Nevertheless, descriptive analyses indicated a higher frequency of renal cysts and structural kidney changes in animals with renal amyloid deposition (odds ratios: 2.19-9.51). Notably, the detection of cysts on gross pathology indicated a significant association with renal amyloid deposition ($p < 0.05$; Table 4).

Table 3. Associations between clinical parameters and renal amyloid deposition in *Tupaia belangeri*

Parameter	Test type	Group A (n)	Group B (n)	statistic	df	P value	P (Holm)	Type of sample
Weight (g)	Welch t-test	5[a]	9[a]	-0.42	7.20	0.69	0.69	Morphometric
Age (week)	Wilcoxon rank-sum	5[a]	9[a]	29	–	0.42	0.85	Demographic
Sex	Fisher t-test	5[a]	9[a]	–	–	0.58	0.85	Demographic
Creatinine (mg/dL)	Welch t-test	5[a]	8[a]	2.25	6.78	0.06	0.36	Blood
Urea (mg/dL)	Welch t-test	4[a]	8[a]	1.06	7.00	0.32	0.99	Blood
ALT (U/L)	Wilcoxon rank-sum	4[a]	7[a]	4.50	–	0.09	0.43	Blood
AST (U/L)	Welch t-test	3[a]	7[a]	-1.25	7.98	0.25	0.99	Blood
TP (g/dL)	Welch t-test	3[a]	8[a]	-0.36	3.88	0.74	1.00	Blood
Alb (g/dL)	Welch t-test	3[a]	7[a]	-0.36	7.99	0.73	1.00	Blood
USG	Welch t-test	5[a]	6[b]	-3.16	7.67	0.01	0.04	Urine
TP urine (g/dL)	Welch t-test	5[a]	6[a]	-1.91	6.02	0.10	0.21	Urine
pH urine	Welch t-test	5[a]	5[a]	0.59	6.06	0.58	0.58	Urine

Comparison of morphometric, demographic, blood, and urine parameters between Group A (with renal amyloid deposition) and Group B (without renal amyloid deposition). ALT: Alanine transaminase, AST: Aspartate transaminase, TP: Total protein, Alb: Albumin, USG: Urine specific gravity, TP urine: Total protein in urine. Data were analyzed using Welch's t-test, Wilcoxon rank-sum test, or Fisher's exact test as appropriate. Reported values included test statistics, degrees of freedom (df), raw P values, and Holm-adjusted P values for multiple comparisons. Values sharing the same superscript letter do not differ significantly; [a,b] mean different superscript letters indicate significant differences in a row at Holm-adjusted ($p < 0.05$).

Table 4. Associations between renal amyloid and renal cysts or sonographic findings in *Tupaia belangeri*

Variable 1	Variable 2	Test type	Statistics	Effect size	P value	Odds ratio	95% CI lower	95% CI upper	P (Holm)
Renal amyloid presence (Group A/ B)	Presence of renal cysts	Fisher	–	–	< 0.01	–	4.48	∞	< 0.01[a]
Renal amyloid presence (Group A/ B)	Presence of cysts in sonography	Fisher	–	–	0.09	9.51	0.49	701.44	0.38
Renal amyloid presence (group A/ B)	Structural changes seen in sonography	Fisher	–	–	0.58	2.19	0.11	45.42	0.58
Renal amyloid presence (group A/ B)	Renal sonographic changes	Fisher	–	–	0.27	4.58	0.30	99.20	0.53
Severe renal amyloid (grade 0 – "+++")	Severity of renal cysts	Spearman	S = 11.1	rho = 0.976	< 0.01	–	–	–	< 0.01[a]
Severe renal amyloid (grade 0 – "+++")	Presence of cysts in sonography	Wilcoxon	W = 7.5	rank-biserial	0.04	–	–	–	0.22
Severe renal amyloid (grade 0 – "+++")	Renal sonographic changes	Wilcoxon	W = 12.5	rank-biserial	0.13	–	–	–	0.40

W: Wilcoxon statistic, rho: Spearman correlation coefficient, rank-biserial: Wilcoxon effect size. Statistical testing was performed to evaluate associations between renal amyloid (presence and severity) and renal cysts or sonographic changes. Renal sonographic changes refer to general alterations in the kidneys, whereas structural changes refer specifically to parenchymal alterations, and renal cysts specifically to the presence of cystic structures. Fisher's exact test was used for binary variables, Spearman's rank correlation for ordinal variables, and the Wilcoxon rank-sum test for comparisons of ordinal versus binary variables. Test statistics, effect sizes, odds ratios (with 95% CI), p values, and Holm-adjusted P-values (P [Holm]) are reported. [a] mean statistically significant difference in a column after Holm–Bonferroni correction ($p < 0.05$).

3.4. Heritability

In both models, the intercept estimates were significantly greater than zero. The heritability estimates for general amyloid deposition and renal amyloid deposition were close to zero, with genetic relatedness accounting for less than 0.02% of the total phenotypic variance in either trait. Estimates of kinship variance, residual variance, and calculated heritability values are provided in Table 5.

Table 5. Parameter estimates from the heritability analysis of amyloid deposition and renal amyloid deposition in the *Tupaia belangeri* breeding colony

Parameter	Amyloid deposition	Renal amyloid
Intercept	0.74 ± 0.10	0.47 ± 0.10
Kinship variance	7.75E-05	2.05E-05
Residual variance	0.44	0.50
Heritability (h^2)	≈ 0.000176	≈ 0.00004

Shown are the model intercepts, estimates of kinship-related variance, residual variance, and the resulting narrow-sense heritability (h^2). Heritability values were derived from the proportion of kinship variance relative to total phenotypic variance.

3.5. Anesthesia

All 14 *T. belangeri* were successfully sedated within five minutes to allow the planned diagnostic procedures (mean induction time = 4.5 minutes, range 3-6 minutes; 95% CI: 3.9-5.1 minutes). The duration of sedation ranged from 32 to 71 minutes (mean = 45 minutes; 95% CI: 39-51 minutes). One individual (number 6) required a supplemental intramuscular dose of the anesthetic combination after 23 minutes. In four additional animals (numbers 8, 11, 13, and 14), isoflurane (1-5%) was administered via a mask toward the end of the procedure to maintain adequate anesthesia. All animals recovered uneventfully within seven minutes, following subcutaneous administration of the reversal agents.

4. Discussion

The present study revealed a high prevalence of AA-amyloid deposition in the kidneys and intestines of a captive population of *T. belangeri*. The current results aligned with the previously reported high prevalence (72%)[12] within this breeding colony, thereby reinforcing earlier findings. However, clinical evaluation did not identify a reliable parameter for the early detection of systemic or renal AA-amyloidosis in this species. The USG was the only clinical parameter that was considerably associated with renal amyloid deposition, with lower values in affected animals (Group A) than in unaffected animals (Group B); however, the reliability and clinical relevance of this finding are limited by the lack of established reference values.

Clinical and laboratory parameters, including blood and further urine analyses, ultrasonography, and radiography, indicated no consistent association with amyloid presence, except for a remarkable association between renal cysts and amyloid deposition.

Amyloid deposits were identified across all age groups and regardless of sex or body weight. As Klein et al.[12] indicated, the kidneys appeared to be a key target organ of systemic amyloidosis in *T. belangeri*. Notably, all animals with renal amyloid also had renal cysts, supporting earlier necropsy-based findings in this colony, where parenchymal atrophy and cyst formation were prominent features associated with amyloid accumulation[12]. The localization of amyloid in the renal medulla and accompanying tubular dilation suggested structural compromise. However, none of the animals demonstrated notable clinical signs indicative of renal dysfunction, such as weight loss, anorexia, polyuria, or polydypsia[12].

Interestingly, intestinal amyloid deposition was more frequently detected than renal involvement, with deposits located predominantly in the lamina propria of the small intestine. The prevalence of intestinal amyloidosis observed in this study (53%) was in contrast to the previous estimate of 19% in *T. belangeri*[19]. Intestinal amyloid is well documented in ruminants[33]. Notably, none of the affected animals exhibited clinical signs of gastrointestinal diseases such as diarrhea, hypoproteinemia, or cachexia, underscoring the largely subclinical presentation of amyloidosis in *T. belangeri*[33].

Despite the pronounced renal pathology observed in some individuals, anesthesia was well tolerated by all animals. The combination of fentanyl, medetomidine, and midazolam provided safe and reliable sedation for clinical data collection in *T. belangeri*.

Ultrasonography identified the majority of cystic lesions that were subsequently confirmed histopathologically. Nevertheless, the small sample size, with only six animals exhibiting renal cysts, four of which were detected sonographically, limits the reliability of these observations. Given the advanced severity of most lesions at the time of examination, it remains unclear whether early or subtle renal alterations associated with amyloidosis can be reliably detected by ultrasound in *T. belangeri*. Overall, the consistent findings in the present study, despite a small dataset, highlighted that ultrasonography could be a highly useful diagnostic tool.

Urine parameters, especially USG, indicated trends toward higher values in amyloid-positive individuals, with USG even reaching remarkable levels after Holm correction. Nevertheless, urine-specific reference values were missing, and inter-individual variance was high. Similarly, blood parameters, including creatinine, urea, AST, ALT, and total protein, exhibited substantial inter-individual variation[9] and frequently fell outside existing reference ranges. This variability complicated interpretation and highlighted the need for broader, species-specific reference intervals.

Although elevated creatinine levels were common, these findings were not consistently associated with amyloid deposition. Variations in blood and urine parameters could potentially be related to the use of anesthetic medicines. In particular, α2-adrenergic agonists such as medetomidine are known to influence renal perfusion, glomerular filtration, and urine concentrating ability, which may affect serum creatinine, urea, and urine specific gravity[35,36].

One animal in the amyloid-positive, Group A (number 15, Quanta), which exhibited renal amyloidosis and renal cysts, was found dead in its cage without preceding clinical signs. Histopathological evaluation revealed a malignant lymphoma infiltrating the liver, kidneys, and heart. Additionally, the second animal (number 14) showed neoplastic changes consistent with malignant lymphoma. Malignant lymphoma has previously been reported in *T. belangeri*[37], which is consistent with the present findings, and the prevalence observed in the present study (11%) suggests that lymphoma may occur with noteworthy frequency in this breeding colony. The presence of malignant lymphoma could potentially contribute to amyloid formation, although this typically involves a different amyloid type than the renal amyloidosis identified in the present study[15].

No evidence was found for a hereditary component underlying amyloid deposition in this breeding colony. Narrow-sense heritability estimated for general and renal amyloidosis was near zero, indicating that additive genetic factors played a minimal role. However, the small sample size limited statistical power, and the model accounted for only additive variance. Given the previously reported high prevalence of amyloidosis in this species[12], and its presence in this colony, amyloidosis appears to be a common finding in *T. belangeri*, which is in alignment with the present findings.

Importantly, amyloidosis has not been reported in wild northern tree shrews. This suggested that captivity may contribute to its development, consistent with findings in other animals, including livestock and zoo populations[17,38]. Two mechanisms have been proposed, including the potential transmissibility of misfolded β-sheeted amyloidogenic proteins and chronic stress as a trigger for amyloidogenesis. While definitive evidence for transmissible AA-amyloidosis is lacking, experimental studies indicate possible inter and even cross-species transmission of amyloidogenic seeds[39,40]. High levels of

amyloidogenic proteins in feces may also increase the risk of environmental transmission[17]. Close housing conditions in this breeding colony could therefore have facilitated exposure and spread.

Chronic stress is a plausible risk factor. It has been linked to increased risk of AA-amyloidosis in production animals, such as commercially raised birds[17], and experimental models have shown that stress exacerbates Aβ pathology[41]. In humans, chronic stress is a well-established risk factor for neuropsychiatric and neurodegenerative diseases and is frequently associated with Hypothalamic–Pituitary–Adrenal–axis dysregulation and elevated cortisol levels[42,43]. *T. belangeri* are known to be particularly susceptible to psychosocial stress, showing marked behavioral and physiological changes under social or territorial stressors, such as forced cohabitation of males[8,44]. Stress-prone behavioral traits in *T. belangeri* might increase the likelihood of amyloidogenic processes in captivity. Markers of physiological stress such as glucocorticoid or cortisol concentrations[45,46], as well as neutrophil-to-lymphocyte ratios[47] may offer valuable insights into stress-related disease susceptibility. In addition, inflammatory biomarkers, including ferritin[48,49], serum amyloid A[50], and fibrinogen[51], could contribute to identifying chronic inflammatory processes that may promote the development of systemic AA-amyloidosis. In the current study, the limited blood volume obtainable from each individual restricted the range of measurable analytes, necessitating a primary focus on clinical indicators of renal function. Furthermore, reference values for chronic disease and inflammatory markers are currently unavailable for *T. belangeri*, which limited a comprehensive assessment of chronic stress and disease dynamics in *T. belangeri*.

The present findings raise important questions about animal welfare. A notable number of the animals, some as young as one year, exhibited moderate to severe systemic amyloidosis. Chronic pathological conditions such as amyloidosis can remain subclinical for extended periods of time, evading detection through routine monitoring, potentially allowing disease progression and associated organ dysfunction before intervention is possible. Additional findings of pododermatitis[52], orthopedic lesions[53], and incidental tumors point towards a multifactorial health burden[54].

The spontaneous development of systemic amyloidosis in *T. belangeri* presented challenges and opportunities. While it may confound studies not targeting amyloid-related disease, it also presented a valuable opportunity to study protein misfolding disorders, such as AA-amyloidosis or systemic inflammation. Their genetic, neuroanatomical, and biochemical similarities to primates[6] make northern tree shrews a compelling but underutilized model. Their limited use to date is likely due to challenges in husbandry, scarcity of species-specific reagents, and a lack of standardized diagnostic tools[9].

Clinically, diagnosing amyloidosis in animals remains difficult, as general diagnostic markers are largely lacking[16]. Most cases are detected post-mortem[13], and the incidence of systemic amyloidosis in animals is likely underreported[13]. Despite its limitations, including a small sample size and variability in reference values, the present study offered crucial preliminary insights. Notably, the consistent finding of renal cysts in amyloid-positive animals reinforced previous observations and may serve as an early indicator of renal involvement.

5. Conclusion

The current study indicated a high occurrence of amyloidosis in the intestines and kidneys of northern captive tree shrews, although it often lacked obvious clinical signs. The present findings underscore the need for more systematic investigations into the environmental and physiological factors driving amyloidogenesis in captivity, particularly the potential roles of chronic stress and transmissible amyloidogenic proteins. Future studies should prioritize methodological refinement, including larger sample sizes, standardized imaging and biochemical protocols, and the establishment of species-specific reference values for blood and urine parameters. From a welfare perspective, the common presence of subclinical but widespread systemic pathology in *T. belangeri* warrants a serious reevaluation of husbandry and breeding practices. At the same time, the spontaneous development of amyloidosis in *T. belangeri* provides a valuable opportunity to study protein misfolding diseases in a translationally relevant model species.

Declarations

Competing interests

The authors declared no competing interests.

Authors' contributions

Natalie Steiner was involved in data analysis and interpretation, drafting, critical revision of the manuscript, and final approval. Tina Brezina was involved in study design, data acquisition, drafting, and revision of the manuscript. Felix Felmy was involved in the study design and manuscript revision. Frederik Kiene was involved in data acquisition, drafting, and revision. Yara Silberstein was involved in data acquisition, drafting, and revision. Malgorzata Ciurkiewicz, Jan Hinrich Bräsen and Reinhold Paul Linke were involved in data acquisition. Claudia Busse was involved in data acquisition and manuscript revision. Andreas Beineke was involved in data acquisition and manuscript revision. Michael Pees was involved in data analysis and revision. Ute Radespiel was involved in study design and revision of the manuscript. Maximilian Reuschel was involved in study design, data acquisition, and drafting and revising the manuscript. All authors checked and approved the final edition of the manuscript.

Funding

This study did not receive any specific grant from funding agencies in the public, commercial, or not-for-profit sectors.

Availability of data and materials

The original contributions presented in the study are included in the article; further inquiries can be directed to the corresponding author.

Acknowledgments

The authors can acknowledge anyone who contributed to the study but does not meet the criteria for authorship.

Ethical considerations

The authors have adhered to ethical standards throughout the preparation of this manuscript. Ethical issues such as plagiarism, duplicate submissions, and data originality were carefully considered and addressed. AI tools, specifically ChatGPT, were used solely for language and grammatical improvements. The authors accept full responsibility for the content, accuracy, and integrity of all AI-assisted text in the manuscript. After using AI (Grammarly) to address grammatical issues, the authors reread and revised the article. All scientific ideas, analyses, conclusions, and statements presented in this study were developed entirely by the authors, who have carefully reviewed and edited all AI-assisted text and accept full responsibility for its content.

References

1. Guimarães AI. Are animal models necessary? Exploring (dis) advantages and alternatives. Eur J Neurosci. 2025; 61(1): e16651. DOI: 10.1111/ejn.16651
2. Wall RJ, and Shani M. Are animal models as good as we think? Theriogenology. 2008; 69(1): 2-9. DOI: 10.1016/j.theriogenology.2007.09.030
3. Perlman RL. Mouse models of human disease: An evolutionary perspective. Evol Med Public Health. 2016; 2016(1): 170-176. DOI: 10.1093/emph/eow014
4. German center for the protection of laboratory animals (Bf3R). Use of laboratory animals in 2023. German Federal Institute for Risk Assessment (BfR). 2025. Available at: https://www.bf3r.de/en/offers/test-animal-numbers/test-animal-numbers-2023/
5. Li R, Xu W, Wang Z, Liang B, Wu JR, and Zeng R. Proteomic characteristics of the liver and skeletal muscle in the Chinese tree shrew (*Tupaia belangeri chinensis*). Protein Cell. 2012; 3(9): 691-700. DOI: 10.1007/s13238-012-2039-0
6. Zheng L, Chen S, Wu Q, Li X, Zeng W, Dong F, et al. Tree shrews as a new animal model for systemic sclerosis research. Front Immunol. 2024;15: 1315198. DOI: 10.3389/fimmu.2024.1315198
7. Xiao J, Liu R, and Chen CS. Tree shrew (*Tupaia belangeri*) as a novel laboratory disease animal model. Zool Res. 2017; 38(3): 127. DOI: 10.24272/j.issn.2095-8137.2017.033
8. Fuchs E. Tree shrews at the German Primate Center. Primate Biol. 2015; 2(1): 111-118. DOI: 10.5194/pb-2-111-2015
9. Yao YG, Lu L, Ni RJ, Bi R, Chen C, Chen JQ, et al. Study of tree shrew biology and models: A booming and prosperous field for biomedical research. Zool Res. 2024; 45(4): 877-909. DOI: 10.24272/j.issn.2095-8137.2024.199
10. Li H, Xiang BL, Li X, Li C, Li Y, Miao Y, et al. Cognitive deficits and Alzheimer's disease-like pathologies in the aged Chinese tree shrew. Mol Neurobiol. 2024; 61(4): 1892-1906. DOI: 10.1007/s12035-023-03663-7
11. Li R, Zanin M, Xia X, and Yang Z. The tree shrew as a model for infectious diseases research. J Thorac Dis. 2018; 10(S9): S2272-S2279. DOI: 10.21037/jtd.2017.12.121
12. Klein A, Radespiel U, Felmy F, Brezina T, Ciurkiewicz M, Schmitz J, et al. AA-amyloidosis in captive northern tree shrews (*Tupaia belangeri*). Vet Pathol. 2022; 59(2): 340-347. DOI: 10.1177/03009858211066847
13. Garg A, and Thakur AK. The worldwide need for amyloid diagnosis in animals. J Biosci. 2023; 48(4): 46. DOI: 10.1007/s12038-023-00372-0
14. Iwaide S, Murakami T, Sedghi Masoud N, Kobayashi N, Fortin JS, Miyahara H, et al. Classification of amyloidosis and protein misfolding disorders in animals 2024: A review on pathology and diagnosis. Vet Pathol. 2024; 62(2): 117-138. DOI: 10.1177/03009858241283750
15. Woldemeskel M. A concise review of amyloidosis in animals. Vet Med Int. 2012; 2012(1): 247296. DOI: 10.1155/2012/427296
16. Rowland H, Blundell R, Chantrey J, Edwards KL, Moss A, Stidworthy MF, et al. Amyloidosis in captive European eastern bongo (*Tragelaphus eurycerus isaaci*): Prevalence, predictive factors, organ predilection, and serum amyloid A concentrations. J Zoo Wildl Med. 2023; 53(4): 696-704. DOI: 10.1638/2022-0048
17. Murakami T, Ishiguro N, and Higuchi K. Transmission of systemic AA amyloidosis in animals. Vet Pathol. 2014; 51(2): 363-371. DOI: 10.1177/0300985813511128
18. Schehka S, and Zimmermann E. Affect intensity in voice recognized by tree shrews (*Tupaia belangeri*). Emotion. 2012; 12(3): 632. DOI: 10.1037/a0026893
19. Albrecht M, Henke J, Tacke S, Markert M, and Guth B. Influence of repeated anaesthesia on physiological parameters in male Wistar rats: A telemetric study about isoflurane, ketamine-xylazine and a combination of medetomidine, midazolam and fentanyl. BMC Vet Res. 2014; 10(1): 310. DOI: 10.1186/s12917-014-0310-8
20. Henke J, Baumgartner C, Röltgen I, Eberspächer E, and Erhardt W. Anaesthesia with midazolam/medetomidine/fentanyl in chinchillas (*Chinchilla lanigera*) compared to anaesthesia with xylazine/ketamine and medetomidine/ketamine. J Vet Med A. 2004; 51(5): 259-264. DOI: 10.1111/j.1439-0442.2004.00632.x
21. Henke J, Astner S, Brill T, Eissner B, Busch R, and Erhardt W. Comparative study of three intramuscular anaesthetic combinations (medetomidine/ketamine, medetomidine/fentanyl/midazolam and xylazine/ketamine) in rabbits. Vet Anaesth Analg. 2005; 32(5): 261-270. DOI: 10.1111/j.1467-2995.2005.00242.x
22. Schmitz S, Tacke S, Guth B, and Henke J. Comparison of physiological parameters and anaesthesia specific observations during isoflurane, ketamine-xylazine or medetomidine-midazolam-fentanyl anaesthesia in male guinea pigs. PLoS ONE. 2016; 11(9): e0161258. DOI: 10.1371/journal.pone.0161258
23. Brezina TE, Reuschel M, Keine F, Silberstein Y, Felmy FC, Fehr M, et al. Einsatz der vollständig antagonisierbaren Anästhesie (Midazolam, Medetomidin und Fentanyl) bei 19 Tupaias (*Tupaia belangeri*) im Rahmen einer Gesundheitsuntersuchung [Use of fully reversible anesthesia (midazolam, medetomidine and fentanyl) in 19 Tupaias (*Tupaia belangeri*) during a health check-up]. Kleintierprax. 2022; 67(8): 468. Available at: https://elib.tiho-hannover.de/receive/tiho_mods_00007961?utm
24. Ma XT, Li FL, Jiang HJ, Li WH, Zhang Y, and Du TY. Detection and comparison of physiological indexes in the wild and laboratory tree shrew. Zool Res. 2011; 1(32): 4-10. DOI: 10.3724/SP.J.1141.2011.01004
25. Zou RJ, Ben KL, and Song BY. Blood picture of the tree shrew (*Tupaia belangeri*). Zool Res. 1983; 4(3): 291-294. Available at: https://zoores.ac.cn/en/article/id/1681
26. Yanzhang P, Zhizhang YE, and Yaopin Z. Biochemical reference values in tree shrews (*Tupaia belangeri chinesis*). Acta Theriol Sin. 1986; 6(2): 1-10. Available at: https://www.mammal.cn/EN/Y1986/V6/I2/115
27. Bakker J, Maaskant A, Wegman M, Zijlmans DG, Hage P, Langermans JA, et al. Reference intervals and percentiles for hematologic and serum biochemical values in captive bred Rhesus (*Macaca mulatta*) and Cynomolgus macaques (*Macaca fascicularis*). Animals. 2023; 13(3): 445. DOI: 10.3390/ani13030445
28. Park HK, Cho JW, Lee BS, Park H, Han JS, Yang MJ, et al. Reference values of clinical pathology parameters in cynomolgus monkeys (*Macaca fascicularis*) used in preclinical studies. Lab Anim Res. 2016; 32(2): 79-86. DOI: 10.5625/lar.2016.32.2.79

29. Linke RP. Monoclonal antibodies against amyloid fibril protein AA. Production, specificity, and use for immunohistochemical localization and classification of AA-type amyloidosis. J Histochem Cytochem. 1984; 32(3): 322-328. DOI: 10.1177/32.3.6363521
30. Therneau T. Mixed effects Cox models. CRAN Repo. 2020. p. 1-14. Available at: http://download.nust.na/pub3/cran/web/packages/coxme/vignettes/coxme.pdf
31. DiBartola SP, Tarr MJ, Parker AT, Powers JD, and Pultz JA. Clinicopathologic findings in dogs with renal amyloidosis: 59 cases (1976-1986). J Am Vet Med Assoc. 1989; 195(3): 358-364. DOI: 10.2460/javma.1989.195.03.358
32. Slauson DO, Gribble DH, and Russell SW. A clinicopathological study of renal amyloidosis in dogs. J Comp Pathol. 1970; 80(2): 335-343. DOI: 10.1016/0021-9975(70)90104-0
33. Biescas E, Jirón W, Climent S, Fernández A, Pérez M, Weiss DT, et al. AA amyloidosis induced in sheep principally affects the gastrointestinal tract. J Comp Pathol. 2009; 140(4): 238-246. DOI: 10.1016/j.jcpa.2008.12.004
34. Talar-Wojnarowska R, and Jamroziak K. Intestinal amyloidosis: Clinical manifestations and diagnostic challenge. Adv Clin Exp Med. 2021; 30(5): 563-570. DOI: 10.17219/acem/133521
35. Pypendop BH, and Verstegen JP. Hemodynamic effects of medetomidine in the dog: A dose titration study. 1998; 27(6): 612-622. DOI: 10.1111/j.1532-950x.1998.tb00539.x
36. Murrell JC, and Hellebrekers LJ. Medetomidine and dexmedetomidine: A review of cardiovascular effects and antinociceptive properties in the dog. Vet Anaesth Analg. 2005; 32(3): 117-127. DOI: 10.1111/j.1467-2995.2005.00233.x
37. Brack M. Spontaneous tumours in tree shrews (*Tupaia belangeri*): population studies. J Comp Pathol. 1998; 118(4): 301-316. DOI: 10.1016/S0021-9975(07)80006-5
38. Ferri F, Ferro S, Porporato F, Callegari C, Guglielmetti C, Mazza M, et al. AA-amyloidosis in cats (*Felis catus*) housed in shelters. PLoS ONE. 2023; 18(3): e0281822. DOI: 10.1371/journal.pone.0281822
39. Tjernberg LO, Rising A, Johansson J, Jaudzems K, and Westermark P. Transmissible amyloid. J Intern Med. 2016; 280(2): 153-163. DOI: 10.1111/joim.12499
40. Westermark GT, and Westermark P. Serum amyloid A and protein AA: Molecular mechanisms of a transmissible amyloidosis. FEBS Lett. 2009; 583(16): 2685-2690. DOI: 10.1016/j.febslet.2009.04.026
41. Morgese MG, Schiavone S, and Trabace L. Emerging role of amyloid beta in stress response: Implication for depression and diabetes. Eur J Pharmacol. 2017; 817: 22-29. DOI: 10.1016/j.ejphar.2017.08.031
42. Green KN, Billings LM, Roozendaal B, McGaugh JL, and LaFerla FM. Glucocorticoids increase amyloid-β and tau pathology in a mouse model of Alzheimer's disease. J Neurosci. 2006; 26(35): 9047-9056. DOI: 10.1523/JNEUROSCI.2797-06.2006
43. Baglietto-Vargas D, Chen Y, Suh D, Ager RR, Rodriguez-Ortiz CJ, Medeiros R, et al. Short-term modern life-like stress exacerbates Aβ-pathology and synapse loss in 3xTg-AD mice. J Neurochem. 2015; 134(5): 915-926. DOI: 10.1111/jnc.13195
44. Holst DV. Renal failure as the cause of death in *Tupaia belangeri* exposed to persistent social stress. J Comp Physiol. 1972; 78(3): 236-273. DOI: 10.1007/BF00697657
45. Collins P, Tsang W, and Metzger J. Influence of stress on adrenocortical function in the male tree shrew (*Tupaia belangeri*). Gen Comp Endocrinol. 1984; 55(3): 450-457. DOI: 10.1016/0016-6480(84)90017-0
46. Meyer U, van Kampen M, Isovich E, Flügge G, and Fuchs E. Chronic psychosocial stress regulates the expression of both GR and MR mRNA in the hippocampal formation of tree shrews. Hippocampus. 2001; 11(3): 329-336. DOI: 10.1002/hipo.1047
47. Davis A, Maney D, and Maerz J. The use of leukocyte profiles to measure stress in vertebrates: A review for ecologists. Funct Ecol. 2008; 22(5): 760-772. DOI: 10.1111/j.1365-2435.2008.01467.x
48. Kell DB, and Pretorius E. Serum ferritin is an important inflammatory disease marker, as it is mainly a leakage product from damaged cells. Metallomics. 2014; 6(4): 748-773. DOI: 10.1039/c3mt00347g
49. Chikazawa S, Nakazawa T, Hori Y, Hoshi F, Kanai K, Ito N, et al. Change in serum ferritin concentration in experimentally induced anemia of chronic inflammation in dogs. J Vet Med Sci. 2013; 75(11): 1419-1426. DOI: 10.1292/jvms.13-0149
50. Den Hartigh LJ, May KS, Zhang XS, Chait A, and Blaser MJ. Serum amyloid A and metabolic disease: Evidence for a critical role in chronic inflammatory conditions. Front Cardiovasc Med. 2023; 10: 1197432. DOI: 10.2746/042516402776250405
51. Hultén C, Grönlund U, Hirvonen J, Tulamo RM, Suominen MM, Marhaug G, et al. Dynamics in serum of the inflammatory markers serum amyloid A (SAA), haptoglobin, fibrinogen and α2-globulins during induced noninfectious arthritis in the horse. Equine Vet J. 2002; 34(7): 699-704. DOI: 10.2746/042516402776250405
52. Blair J. Bumblefoot: A comparison of clinical presentation and treatment of pododermatitis in rabbits, rodents, and birds. Vet Clin North Am Exot Anim Pract. 2013; 16(3): 715-735. DOI: 10.1016/j.cvex.2013.05.002
53. Grosso FV. Orthopedic diagnostic imaging in exotic pets. Vet Clin North Am Exot Anim Pract. 2019; 22(2): 149-173. DOI: 10.1016/j.cvex.2019.01.003
54. Reavill DR, and Imai DM. Pathology of diseases of geriatric exotic mammals. Vet Clin North Am Exot Anim Pract. 2020; 23(3): 651-684. DOI: 10.1016/j.cvex.2020.06.002

Table S1. Overview of all *Tupaia belangeri* included in the present study

Animal ID	Sex	Age (year)	Group	Date of examination 1	Date of examination 2	Date of necropsy	Days until necropsy
1	M	5	A	24.02.2021	Not performed	11.03.2021	15
2	F	1	A	20.01.2021	14.07.2021	20.07.2021	6
3	F	3	A	04.02.2021	Not performed	09.02.2021	5
4	F	3	A	04.02.2021	09.06.2021	17.06.2021	8
5	F	4	A	11.02.2021	20.05.2021	20.05.2021	0
6	M	1	B	03.02.2021	14.07.2021	19.07.2021	5
7	M	1	B	13.01.2021	23.06.2021	24.06.2021	1
8	M	5	B	24.02.2021	Not performed	10.03.2021	14
9	M	5	B	11.02.2021	19.05.2021	19.05.2021	0
10	F	1	B	13.01.2021	15.07.2021	21.07.2021	6
11	F	3	B	20.01.2021	09.06.2021	16.06.2021	7
12	F	3	B	11.02.2021	Not performed	26.02.2021	15
13	F	2	B	11.02.2021	07.06.2021	08.06.2021	1
14	F	4	B	24.02.2021	07.06.2021	10.06.2021	3
15	F	5	A	13.01.2021	Not performed	08.04.2021	81
16	M	4	A	13.01.2021	Not performed	04.03.2021	50
17	F	4	A	04.02.2021	Not performed	01.03.2021	25
18	F	5	A	20.01.2021	Not performed	25.02.2021	36
19	M	5	B	20.01.2021	Not performed	22.02.2021	33

Animals 15-19: Used exclusively for pathological investigation, as the interval between clinical examination and necropsy exceeded 15 days. Group A: Animals that are classified as amyloid-positive based on the presence of renal amyloid deposits, Group B: Animals that are classified as amyloid-negative with no renal amyloid deposition. F: Female, M: Male.

Table S2. Overview of ultrasonographic changes in relation to amyloid deposits in *Tupaia belangeri*

Animal ID	Group	Amyloid deposition	Renal amyloid grading	Renal cysts grading	US renal cysts (Y/N)	US renal parenchymal changes (Y/N)
1	A	1	++	++	Y	Y
2	A	1	++	+	Y	N
3	A	2	++	+++	Y	Y
4	A	2	+	+	N	N
5	A	3	++	+	N	N
6	B	0	0	0	N	N
7	B	0	0	0	N	N
8	B	0	0	0	N	Y
9	B	1	0	0	Y	Y
10	B	0	0	0	N	N
11	B	1	0	0	N	N
12	B	1	0	0	N	N
13	B	2	0	0	N	N
14	B	3	0	0	N	N
15	A	2	++	+	-	-
16	A	2	+	++	-	-
17	A	1	++	+	-	-
18	A	2	+++	+++	-	-
19	B	0	0	+++	-	-

Group A: Animals classified as amyloid-positive based on the presence of amyloid deposits in the kidneys, Group B: Animals considered as amyloid-negative with no renal amyloid deposition. The column amyloid deposition indicated the number of organ systems in which amyloid was detected: 0: Absent, 1: Present in a single location, 2: Present in two locations, 3: Present in three or more locations. Renal amyloidosis and renal cysts were graded using a semiquantitative scoring system[12]. Renal amyloid grading: 0: Absent, +: Mild (scattered deposits in the renal papilla; <10% of the renal medulla affected), ++: Moderate (10-50% of the renal medulla affected), +++: Severe (>50% of the renal medulla affected). Renal cyst grading: 0: Absent, +: Sporadic/few cysts, ++: Multiple cysts, +++: Numerous cysts with prominent atrophy of the renal parenchyma. -: Not assessed. US: Ultrasonographic findings include the presence or absence of renal cysts (US renal cysts) and renal parenchymal changes (US renal parenchymal changes) and are indicated as yes (Y) or no (N).

Table S3. Histopathological changes observed in all *Tupaia belangeri* examined

Animal ID	Group	Date of necropsy	Amyloid deposition	Grading renal amyloid	Grading renal cysts
1	A	11.03.2021	Kidney	-	++
2	A	20.07.2021	Kidney	++	+
3	A	09.02.2021	Kidney, intestine	++	+++
4	A	17.06.2021	Kidney, intestine	+	+
5	A	20.05.2021	Kidney, intestine, heart valve	++	+
6	B	19.07.2021	Not present	-	-
7	B	24.06.2021	Not present	-	-
8	B	10.03.2021	Not present	-	-
9	B	19.05.2021	Intestine	-	-
10	B	21.07.2021	Not present	-	-
11	B	16.06.2021	Intestine	-	-
12	B	26.02.2021	Intestine	-	-
13	B	08.06.2021	Intestine, lungs	-	-
14	B	10.06.2021	lungs, uterus, intestine	++	-
15	A	08.04.2021	Kidney, intestine	+	++
16	A	04.03.2021	Kidney, intestine	+	++
17	A	01.03.2021	Kidney	++	+
18	A	25.02.2021	Kidney, intestine	+++	+++
19	B	22.02.2021	-	-	+++

Renal amyloidosis and renal cysts were graded using a semiquantitative approach Klein et al.12. Group A: Animals classified as amyloid-positive based on the presence of amyloid deposits in the kidneys, Group B: Animals considered as amyloid-negative with no renal amyloid deposition. Renal amyloid grading: 0: Absent, +: Mild (scattered deposits in the renal papilla; <10% of the renal medulla affected), ++: Moderate (10-50% of the renal medulla affected), +++: Severe (>50% of the renal medulla affected). Renal cyst grading: 0: Absent, +: Sporadic/few cysts, ++: Multiple cysts, +++: Numerous cysts with prominent atrophy of the renal parenchyma.